

Bigger is not Always Better: Scaling Properties of Latent Diffusion Models

Kangfu Mei*^{1,2}, Zhengzhong Tu¹, Mauricio Delbracio¹,
Hossein Talebi¹, Vishal M. Patel², Peyman Milanfar¹

¹ Google Research

² Johns Hopkins University

Abstract. We study the scaling properties of latent diffusion models (LDMs) with an emphasis on their sampling efficiency. While improved network architecture and inference algorithms have shown to effectively boost sampling efficiency of diffusion models, the role of model size—a critical determinant of sampling efficiency—has not been thoroughly examined. Through empirical analysis of established text-to-image diffusion models, we conduct an in-depth investigation into how model size influences sampling efficiency across varying sampling steps. Our findings unveil a surprising trend: when operating under a given inference budget, smaller models frequently outperform their larger equivalents in generating high-quality results. Moreover, we extend our study to demonstrate the generalizability of these findings by applying various diffusion samplers, exploring diverse downstream tasks, evaluating post-distilled models, as well as comparing performance relative to training compute. These findings open up new pathways for the development of LDM scaling strategies which can be employed to enhance generative capabilities within limited inference budgets.

Keywords: Scaling Properties · Latent Diffusion Models

1 Introduction

Latent diffusion models (LDMs) [55], and diffusion models in general, trained on large-scale, high-quality data [30, 62] have emerged as a powerful and robust framework for generating impressive results in a variety of tasks, including image synthesis and editing [9, 48, 49, 53, 55], video creation [42, 43, 63, 70], audio production [31], and 3D synthesis [28, 32]. Despite their versatility, the major barrier against wide deployment in real-world applications [8, 12] comes from their low *sampling efficiency*. The essence of this challenge lies in the inherent reliance of LDMs on multi-step sampling [16, 66] to produce high-quality outputs, where the total cost of sampling is the product of sampling steps and the cost of each step. Specifically, the go-to approach involves using the 50-step DDIM sampling [55, 64], a process that, despite ensuring output quality, still

* This work was done during an internship at Google

requires a relatively long latency for completion on modern mobile devices with post-quantization. In contrast to single shot generative models (e.g., generative-adversarial networks (GANs) [13]) which bypass the need for iterative refinement [13, 23], the operational latency of LDMs calls for a pressing need for efficiency optimization to further facilitate their practical applications.

Recent advancements in this field [8, 24, 25, 27, 47, 74] have primarily focused on developing faster network architectures with comparable model size to reduce the inference time per step, along with innovations in improving sampling algorithms that allow for using less sampling steps [11, 22, 33, 34, 64, 71]. Further progress has been made through diffusion-distillation techniques [14, 36, 41, 59, 61, 65], which simplifies the process by learning multi-step sampling results in a single forward pass, and then broadcasts this single-step prediction multiple times. These distillation techniques leverage the redundant learning capability in LDMs, enabling the distilled models to assimilate additional distillation knowledge. Despite these efforts being made to improve diffusion models, the sampling efficiency of smaller, less redundant models has not received adequate attention. A significant barrier to this area of research is the scarcity of available modern accelerator clusters [20], as training high-quality text-to-image (T2I) LDMs from scratch is both time-consuming and expensive—often requiring several weeks and hundreds of thousands of dollars.

In this paper, we empirically investigate the scaling properties of LDMs, with a particular focus on understanding how their scaling properties impact the sampling efficiency across various model sizes. We trained a suite of 12 text-to-image LDMs from scratch, ranging from 39 million to 5 billion parameters, under a constrained budget. Example results are depicted in Fig. 1. All models were trained on TPUv5 using internal data sources with about 600 million aesthetically-filtered text-to-image pairs. Our study reveals that there exist a scaling trend within LDMs, notably that smaller models may have the capability to surpass larger models under an equivalent sampling budget. Furthermore, we investigate how the size of pre-trained text-to-image LDMs affects their sampling efficiency across diverse downstream tasks, such as real-world super-resolution [57, 58] and subject-driven text-to-image synthesis (i.e., Dreambooth) [56].

1.1 Summary

Our key findings for scaling latent diffusion models in text-to-image generation and various downstream tasks are as follows:

Pretraining performance scales with training compute. We demonstrate a clear link between compute resources and LDM performance by scaling models from 39 million to 5 billion parameters. This suggests potential for further improvement with increased scaling. See Section 3.1 for details.

Downstream performance scales with pretraining. We demonstrate a strong correlation between pretraining performance and success in downstream tasks. Smaller models, even with extra training, cannot fully bridge the gap cre-

ated by the pretraining quality of larger models. This is explored in detail in Section 3.2.

Smaller models sample more efficient. Smaller models initially outperform larger models in image quality for a given sampling budget, but larger models surpass them in detail generation when computational constraints are relaxed. This is further elaborated in Section 3.3 and Section 3.3.

Sampler does not change the scaling efficiency. Smaller models consistently demonstrate superior sampling efficiency, regardless of the diffusion sampler used. This holds true for deterministic DDIM [64], stochastic DDPM [16], and higher-order DPM-Solver++ [35]. For more details, see Section 3.4.

Smaller models sample more efficient on the downstream tasks with fewer steps. The advantage of smaller models in terms of sampling efficiency extends to the downstream tasks when using less than 20 sampling steps. This is further elaborated in Section 3.5.

Diffusion distillation does not change scaling trends. Even with diffusion distillation, smaller models maintain competitive performance against larger distilled models when sampling budgets are constrained. This suggests distillation does not fundamentally alter scaling trends. See Section 3.6 for in-depth analysis.

2 Related Work

Scaling laws. Recent Large Language Models (LLMs) including GPT [3], PaLM [2], and LLaMa [67] have dominated language generative modeling tasks. The foundational works [3, 18, 21] for investigating their scaling behavior have shown the capability of predicting the performance from the model size. They also investigated the factors that affect the scaling properties of language models, including training compute, dataset size and quality, learning rate schedule, etc. Those experimental clues have effectively guided the later language model development, which have led to the emergence of several parameter-efficient LLMs [1, 18, 67, 75]. However, scaling generative text-to-image models are relatively unexplored, and existing efforts have only investigated the scaling properties on small datasets or small models, like scaling UNet [46] to 270 million parameters and DiT [47] on ImageNet (14 million), or less-efficient autoregressive models [6]. Different from these attempts, our work investigates the scaling properties by scaling down the efficient and capable diffusion models, *i.e.* LDMs [55], on internal data sources that have about 600 million aesthetics-filtered text-to-image pairs for featuring the sampling efficiency of scaled LDMs. We also scale LDMs on various scenarios such as finetuning LDMs on downstream tasks [56, 69] and distilling LDMs [41] for faster sampling to demonstrate the generalizability of the scaled sampling-efficiency.

Efficient diffusion models. Nichol et al. [46] show that the generative performance of diffusion models improves as the model size increases. Based on this

Params	39M	83M	145M	223M	318M	430M	558M	704M	866M	2B	5B
Filters (c)	64	96	128	160	192	224	256	288	320	512	768
GFLOPS	25.3	102.7	161.5	233.5	318.5	416.6	527.8	652.0	789.3	1887.5	4082.6
Norm. Cost	0.07	0.13	0.20	0.30	0.40	0.53	0.67	0.83	1.00	2.39	5.17
FID ↓	25.30	24.30	24.18	23.76	22.83	22.35	22.15	21.82	21.55	20.98	20.14
CLIP ↑	0.305	0.308	0.310	0.310	0.311	0.312	0.312	0.312	0.312	0.312	0.314

Table 1: We scale the baseline LDM (*i.e.*, 866M Stable Diffusion v1.5) by changing the base number of channels c that controls the rest of the U-Net architecture as $[c, 2c, 4c, 4c]$ (See Fig. 2). GFLOPS are measured for an input latent of shape $64 \times 64 \times 4$ with FP32. We also show a normalized running cost with respect to the baseline model. The text-to-image performance (FID and CLIP scores) for our scaled LDMs is evaluated on the COCO-2014 validation set with 30k samples, using 50-step DDIM sampling. It is worth noting that all the model sizes, and the training and the inference costs reported in this work only refer to the denoising UNet in the latent space, and do not include the 1.4B text encoder and the 250M latent encoder and decoder.

preliminary observation, the model size of widely used LDMs, *e.g.*, Stable Diffusion [55], has been empirically increased to billions of parameters [48, 51]. However, such a large model makes it impossible to fit into the common inference budget of practical scenarios. Recent work on improving the sampling efficiency focus on improving network architectures [8, 24, 25, 27, 47, 74] or the sampling procedures [11, 22, 33, 34, 64, 71]. We explore sampling efficiency by training smaller, more compact LDMs. Our analysis involves scaling down the model size, training from scratch, and comparing performance at equivalent inference cost.

Efficient non-diffusion generative models. Compared to diffusion models, other generative models such as, Variational Autoencoders (VAEs) [26, 39, 54, 68], Generative Adversarial Networks (GANs) [13, 23, 40, 45, 52], and Masked Models [4, 5, 10, 15, 50], are more efficient, as they rely less on an iterative refinement process. Sauer et al. [60] recently scaled up StyleGAN [23] into 1 billion parameters and demonstrated the single-step GANs’ effectiveness in modeling text-to-image generation. Chang et al. [4] scaled up masked transformer models for text-to-image generation. These non-diffusion generative models can generate high-quality images with less inference cost, which require fewer sampling steps than diffusion models and autoregressive models, but they need more parameters, *i.e.*, 4 billion parameters.

3 Scaling LDMs

We developed a family of powerful Latent Diffusion Models (LDMs) built upon the widely-used 866M Stable Diffusion v1.5 standard [55]³. The denoising UNet of our models offers a flexible range of sizes, with parameters spanning from 39M to 5B. We incrementally increase the number of filters in the residual blocks

³ We adopted SD v1.5 since it is among the most popular diffusion models <https://huggingface.co/models?sort=likes>.

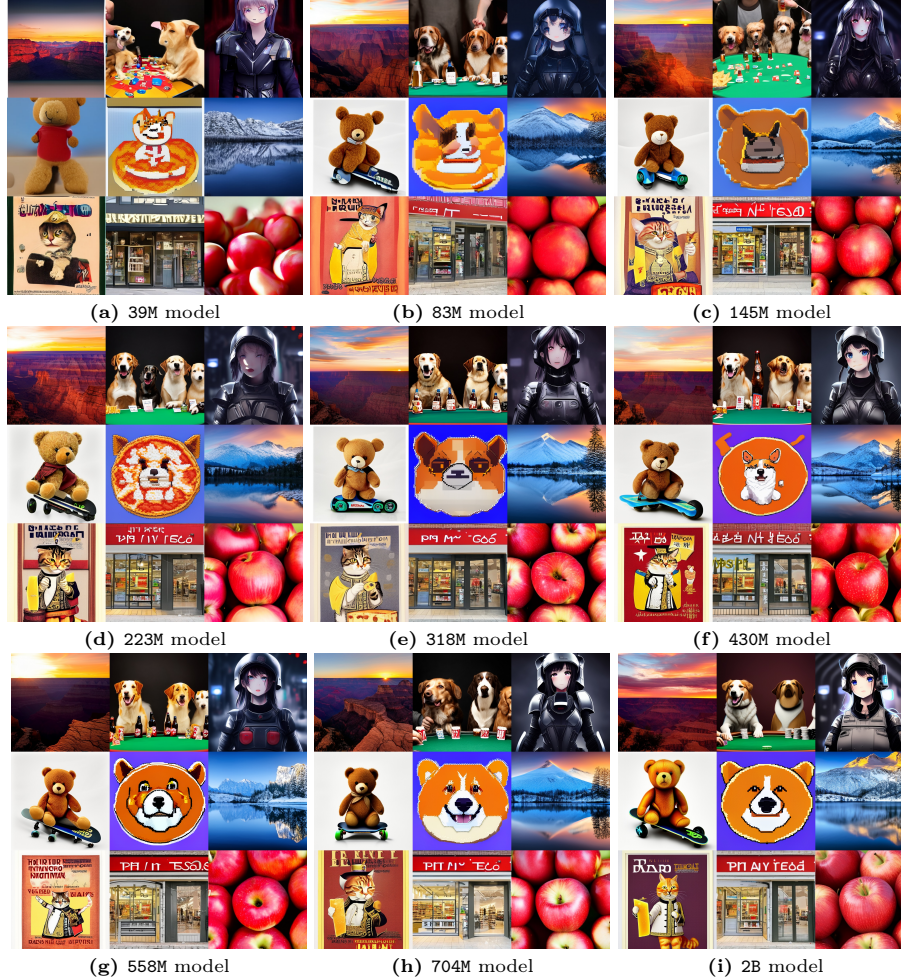


Fig. 1: Text-to-image results from our scaled LDMs (39M - 2B), highlighting the improvement in visual quality with increased model size (note: 39M model is the exception). All images generated using 50-step DDIM sampling. We use representative prompts from PartiPrompts [72], including “a professional photo of a sunset behind the grand canyon.”, “Dogs sitting around a poker table with beer bottles and chips. Their hands are holding cards.”, “Portrait of anime girl in mechanic armor in night Tokyo.”, “a teddy bear on a skateboard.”, “a pixel art corgi pizza.”, “Snow mountain and tree reflection in the lake.”, “a propaganda poster depicting a cat dressed as french emperor napoleon holding a piece of cheese.”, “a store front that has the word ‘LDMs’ written on it.”, and “ten red apples.”. Check our supplement for additional visual comparisons.

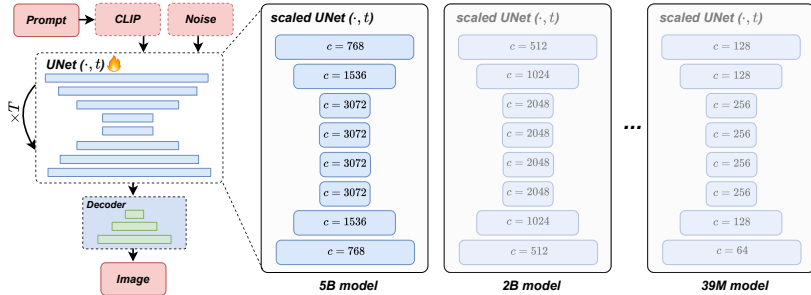


Fig. 2: Our scaled latent diffusion models vary in the number of filters within the denoising U-Net. Other modules remain consistent. Smooth channel scaling (64 to 768) within residual blocks yields models ranging from 39M to 5B parameters. For downstream tasks requiring image input, we use an encoder to generate a latent code; this code is then concatenated with the noise vector in the denoising U-Net.

while maintaining other architecture elements the same, enabling a predictably controlled scaling. Table 1 shows the architectural differences among our scaled models. We also provide the relative cost of each model against the baseline model. Fig. 2 shows the architectural differences during scaling. Models were trained using internal data sources with about 600 million aesthetically-filtered text-to-image pairs. All the models are trained for 500K steps, batch size 2048, and learning rate $1e-4$. This allows for all the models to have reached a point where we observe diminishing returns. Fig. 1 demonstrates the consistent generation capabilities across our scaled models. We used the common practice of 50 sampling steps with the DDIM sampler, 7.5 classifier-free guidance rate, for text-to-image generation. The visual quality of the results exhibits a clear improvement as model size increases.

In order to evaluate the performance of the scaled models, we test the text-to-image performance of scaled models on the validation set of COCO 2014 [30] with 30k samples. For downstream performance, specifically real-world super-resolution, we test the performance of scaled models on the validation of DIV2K with 3k randomly cropped patches, which are degraded with the RealESRGAN degradation [69].

3.1 Training compute scales text-to-image performance

We find that our scaled LDMs, across various model sizes, exhibit similar trends in generative performance relative to training compute cost, especially after training stabilizes, which typically occurs after 200K iterations. These trends demonstrate a smooth scaling in learning capability between different model sizes. To elaborate, Fig. 3 illustrates a series of training runs with models varying in size from 39 million to 5 billion parameters, where the training compute cost is quantified as the product of relative cost shown in Table 1 and training

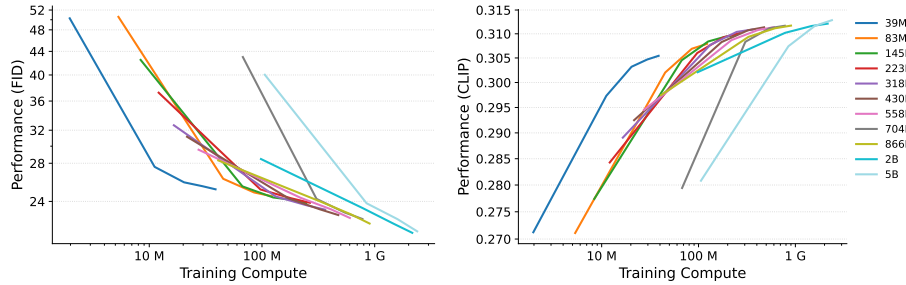


Fig. 3: In text-to-image generation, we observe consistent trends across various model sizes in how quality metrics (FID and CLIP scores) relate to training compute (*i.e.*, the product of training steps and model GFLOPS). Under moderate training resources ($< 1G$) training compute is the most relevant factor dominating quality. When training compute is unlimited (e.g., $\geq 1G$), larger models ($> 700M$) lead to superior performance. Note that the 5B model’s size exceeds single TPU capacity, forcing memory-efficient training. This regime has different learning dynamics than smaller models (e.g., 2B), impacting accuracy at comparable training compute.

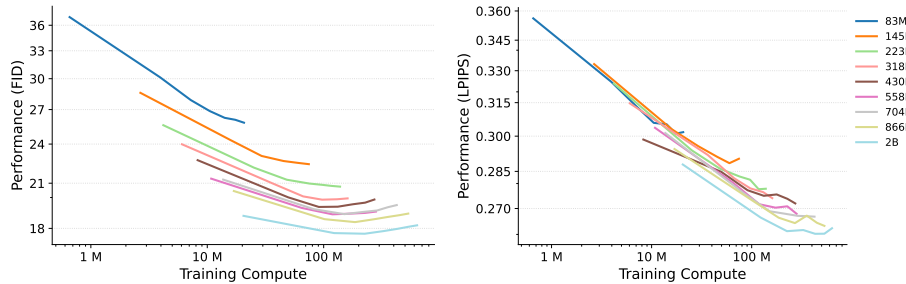


Fig. 4: In $4\times$ real image super-resolution, FID and LPIPS scores reveal an interesting divergence. Model size drives FID improvement, while training compute most impacts LPIPS. Despite this, visual assessment (Fig. 5) confirms the importance of model size for superior detail recovery (similarly as observed in the text-to-image pretraining).

iterations. Model performance is evaluated by using the same sampling steps and sampling parameters. In scenarios with moderate training compute (*i.e.*, $< 1G$, see Fig. 3), the generative performance of T2I models scales well with additional compute resources.

3.2 Pretraining scales downstream performance

Using scaled models based on their pretraining on text-to-image data, we fine-tune these models on the downstream tasks of real-world super-resolution [57, 58] and DreamBooth [56]. The performance of these pretrained models is shown in Table. 1. In the left panel of Fig. 4, we present the generative performance FID versus training compute on the super-resolution (SR) task. It can be seen that the performance of SR models is more dependent on the model size than training compute. Our results demonstrate a clear limitation of smaller models: they

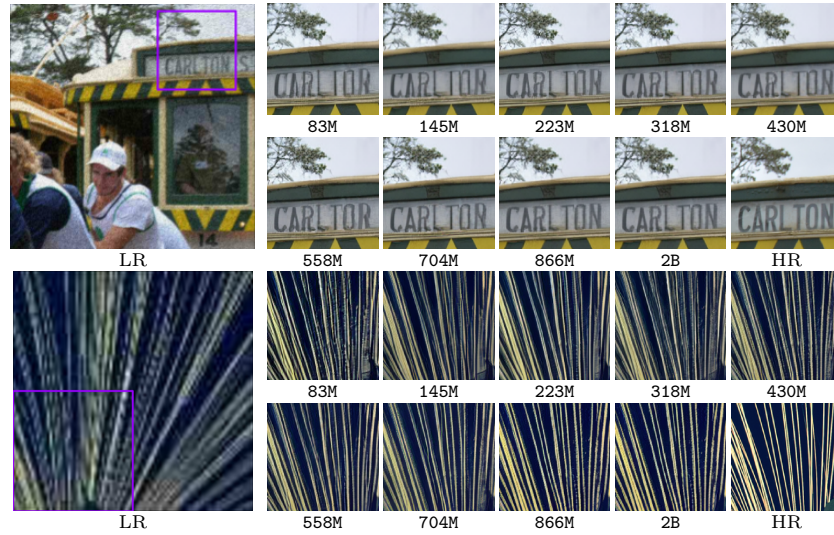


Fig. 5: In $4\times$ super-resolution, visual quality directly improves with increased model size. As these scaled models vary in pretraining performance, the results clearly demonstrate that pretraining boosts super-resolution capabilities in both quantitative (Fig 4) and qualitative ways. *Additional results are given in supplementary material.*

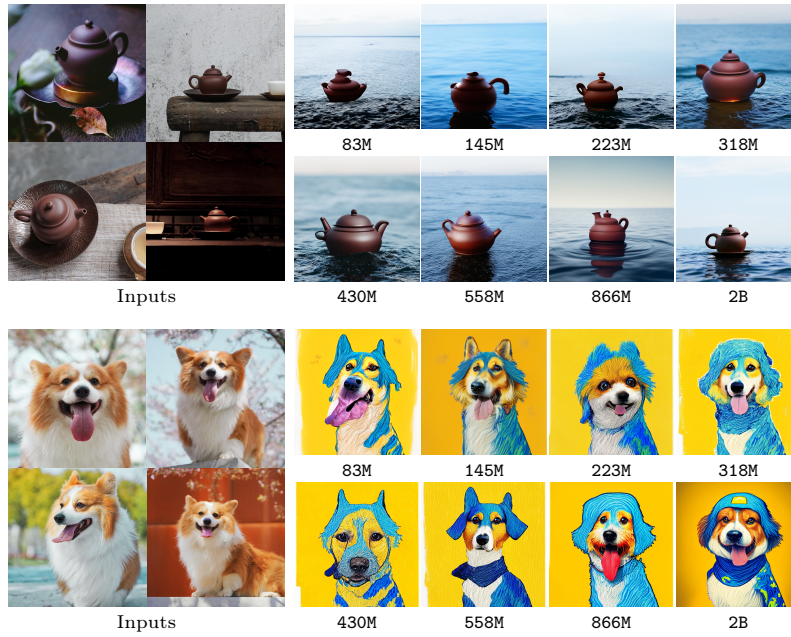


Fig. 6: Visualization of the Dreambooth results shows two distinct tiers based on model size. Smaller models (83M-223M) perform similarly, as do larger ones (318M-2B), with a clear quality advantage for the larger group. *Additional results are given in supplementary material.*

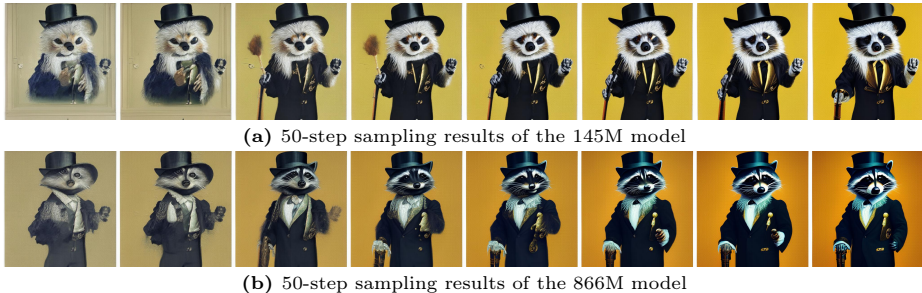


Fig. 7: Visualization of text-to-image results with different CFG rates (from left to right in each row: (1.5, 2.0, 3.0, 4.0, 5.0, 6.0, 7.0, 8.0)). The prompt used is “A raccoon wearing formal clothes, wearing a top hat and holding a cane. Oil painting in the style of Rembrandt.”. We observe that changes in CFG rates impact visual quality more significantly than the prompt semantic accuracy. We use the FID score for quantitative determination of optimal sampling performance (Fig. 8) because it directly measures visual quality, unlike the CLIP score, which focuses on semantic similarity.

cannot reach the same performance levels as larger models, regardless of training compute.

While the distortion metric LPIPS shows some inconsistencies compared to the generative metric FID (Fig. 4), Fig. 5 clearly demonstrates that larger models excel in recovering fine-grained details compared to smaller models.

The key takeaway from Fig. 4 is that large super-resolution models achieve superior results even after short finetuning periods compared to smaller models. This suggests that pretraining performance (dominated by the pretraining model sizes) has a greater influence on the super-resolution FID scores than the duration of finetuning (*i.e.*, training compute for finetuning).

Furthermore, we compare the visual results of the DreamBooth finetuning on the different models in Fig. 6. We observe a similar trend between visual quality and model size. *Please see our supplement for more discussions on the other quality metrics.*

3.3 Scaling sampling-efficiency

Analyzing the effect of CFG rate. Text-to-image generative models require nuanced evaluation beyond single metrics. Sampling parameters are vital for customization, with the Classifier-Free Guidance (CFG) rate [17] directly influencing the balance between visual fidelity and semantic alignment with text prompt. Rombach et al. [55] experimentally demonstrate that different CFG rates result in different CLIP and FID scores.

In this study, we find that CFG rate as a sampling parameter yields inconsistent results across different model sizes. Hence, it is interesting to quantitatively determine the *optimal* CFG rate for each model size and sampling steps using either FID or CLIP score. We demonstrate this by sampling the scaled models using different CFG rates, *i.e.*, (1.5, 2.0, 3.0, 4.0, 5.0, 6.0, 7.0, 8.0)

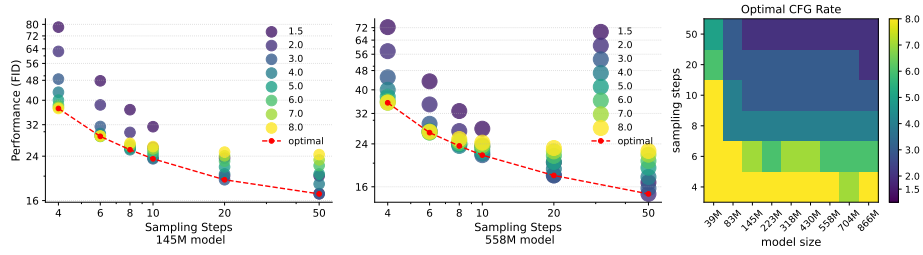


Fig. 8: The impact of the CFG rate on text-to-image generation depends on the model size and sampling steps. As demonstrated in the left and center panels, the optimal CFG rate changes as the sampling steps increased. To determine the optimal performance (according to the FID score) of each model and each sampling steps, we systematically sample the model at various CFG rates and identify the best one. As a reference of the optimal performance, the right panel shows the CFG rate corresponding to the optimal performance of each model for a given number of sampling steps.

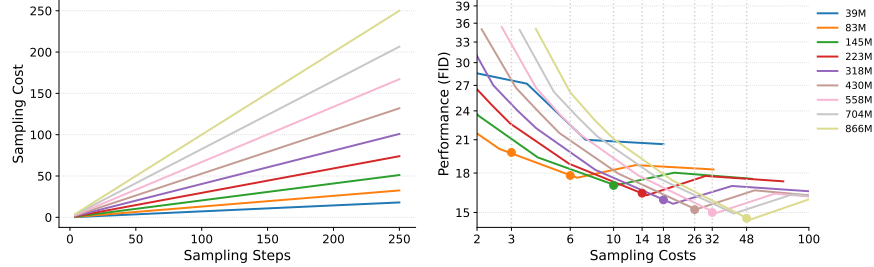


Fig. 9: Comparison of text-to-image performance of models with varying sizes. The left figure shows the relationship between sampling cost (normalized cost \times sampling steps) and sampling steps for different model sizes. The right figure plots the text-to-image FID score as a function of the sampling cost for the same models. Key Observation: Smaller models achieve better FID scores than larger models for a fixed sampling cost. For instance, at a cost of 3, the 83M model achieves the best FID compared to the larger models. This suggests that smaller models might be more efficient in achieving good visual quality with lower costs. We highlight the best performing model at different sampling costs [3–48].

and comparing their quantitative and qualitative results. In Fig. 7, we present visual results of two models under varying CFG rates, highlighting the impact on the visual quality. We observed that changes in CFG rates impact visual quality more significantly than prompt semantic accuracy and therefore opted to use the FID score for quantitative determination of the optimal CFG rate performance. Fig. 8 shows how different classifier-free guidance rates affect the FID scores in text-to-image generation (see figure caption for more details).

Scaling efficiency trends. Using the optimal CFG rates established for each model at various number of sampling steps, we analyze the optimal performance to understand the sampling efficiency of different LDM sizes. Specifically, in

(a) Prompt: “A corgi’s head depicted as a nebula.”. Sampling Cost ≈ 6 .(b) Prompt: “A pineapple surfing on a wave.”. Sampling Cost ≈ 12 .

Fig. 10: Text-to-image results of the scaled LDMs under approximately the same inference cost (normalized cost \times sampling steps). Smaller models can produce comparable or even better visual results than larger models under similar sampling cost.

Fig. 9, we present a comparison between different models and their optimal performance given the sampling cost (normalized cost \times sampling steps). By tracing the points of optimal performance across various sampling cost—represented by the dashed vertical line—we observe a consistent trend: smaller models frequently outperform larger models across a range of sampling cost in terms of FID scores. Furthermore, to visually substantiate better-quality results generated by smaller models against larger ones, Fig. 10 compares the results of different scaled models, which highlights that the performance of smaller models can indeed match their larger counterparts under similar sampling cost conditions. *Please see our supplement for more visual comparisons.*

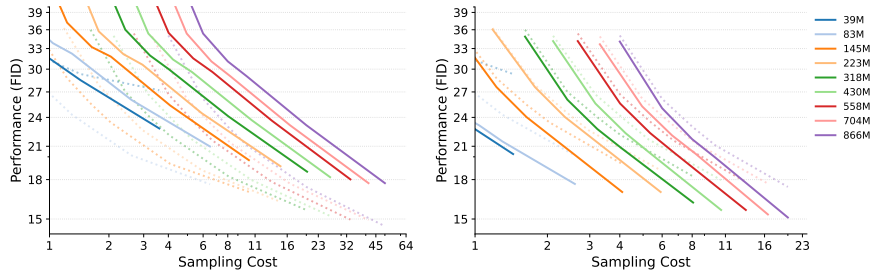


Fig. 11: *Left:* Text-to-image performance FID as a function of the sampling cost (normalized cost \times sampling steps) for the DDPM sampler (solid curves) and the DDIM sampler (dashed curves). *Right:* Text-to-image performance FID as a function of the sampling cost for the second-order DPM-Solver++ sampler (solid curves) and the DDIM sampler (dashed curves). Suggested by the trends shown in Fig. 9, we only show the sampling steps ≤ 50 as using more steps does not improve the performance.

3.4 Scaling sampling-efficiency in different samplers

To assess the generalizability of observed scaling trends in sampling efficiency, we compared scaled LDM performance using different diffusion samplers. In addition to the default DDIM sampler, we employed two representative alternatives: the stochastic DDPM sampler [16] and the high-order DPM-Solver++ [35].

Experiments illustrated in Fig. 11 reveal that the DDPM sampler typically produces lower-quality results than DDIM with fewer sampling steps, while the DPM-Solver++ sampler generally outperforms DDIM in image quality (see the figure caption for details). Importantly, we observe consistent sampling-efficiency trends with the DDPM and DPM-Solver++ sampler as seen with the default DDIM: smaller models tend to achieve better performance than larger models under the same sampling cost. Since the DPM-Solver++ sampler is not designed for use beyond 20 steps, we focused our testing within this range. This finding demonstrates that the scaling properties of LDMs remain consistent regardless of the diffusion sampler used.

3.5 Scaling downstream sampling-efficiency

Here, we investigate the scaling sampling-efficiency of LDMs on downstream tasks, specifically focusing on the super-resolution task. Unlike our earlier discussions on optimal sampling performance, there is limited literature demonstrating the positive impacts of SR performance without using classifier-free guidance. Thus, our approach directly uses the SR sampling result without applying classifier-free guidance. Inspired from Fig. 4, where the scaled downstream LDMs have significant performance difference in 50-step sampling, we investigate sampling efficiency from two different aspects, *i.e.*, fewer sampling steps [4, 20] and more sampling steps (20, 250]. As shown in the left part of Fig. 12, the scaling sampling-efficiency still holds in the SR tasks when the number of sampling steps is less than or equal to 20 steps. Beyond this threshold, however,

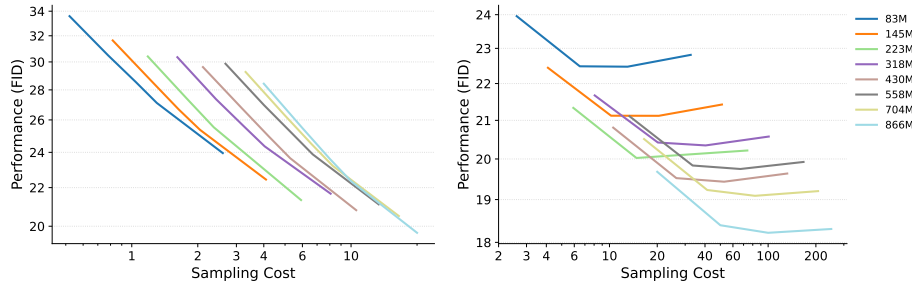


Fig. 12: Super-resolution performance vs. sampling cost for different model sizes. *Left:* FID scores of super-resolution models under limited sampling steps (less than or equal to 20). Smaller models tend to achieve lower (better) FID scores within this range. *Right:* FID scores of super-resolution models under a larger number of sampling steps (greater than 20). Performance differences between models become less pronounced as sampling steps increase.

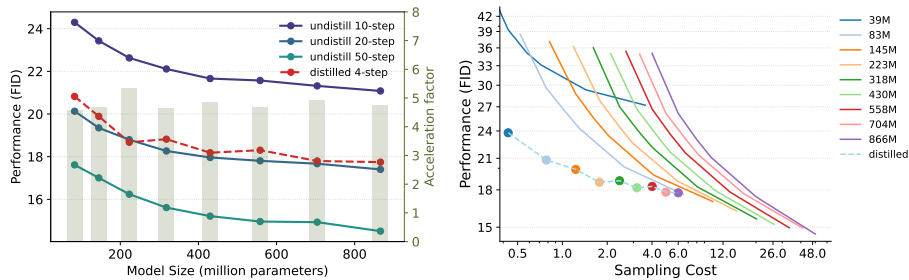


Fig. 13: Distillation improves text-to-image performance and scalability. *Left:* Distilled Latent Diffusion Models (LDMs) consistently exhibit lower (better) FID scores compared to their undistilled counterparts across varying model sizes. The consistent acceleration factor (approx. $5\times$) indicates that the benefits of distillation scale well with model size. *Right:* Distilled models using only 4 sampling steps achieve FID scores comparable to undistilled models using significantly more steps. Interestingly, at a sampling cost of 7, the distilled 866M model performs similarly to the smaller, undistilled 83M model, suggesting improved efficiency. *See the supplement for visual examples demonstrating the quality improvements achieved through distillation.*

larger models demonstrate greater sampling-efficiency than smaller models, as illustrated in the right part of Fig. 12. This observation suggests the consistent sampling efficiency of scaled models on fewer sampling steps from text-to-image generation to super-resolution tasks.

3.6 Scaling sampling-efficiency in distilled LDMs.

We have featured the scaling sampling-efficiency of latent diffusion models, which demonstrates that smaller model sizes exhibit higher sampling efficiency. A notable caveat, however, is that smaller models typically imply reduced mod-

eling capability. This poses a challenge for recent diffusion distillation methods [14, 29, 36, 37, 41, 59, 61, 65] that heavily depend on modeling capability. One might expect a contradictory conclusion and believe the distilled large models sample faster than distilled small models. In order to demonstrate the sampling efficiency of scaled models after distillation, we distill our previously scaled models with conditional consistency distillation [41, 65] on text-to-image data and compare those distilled models on their optimal performance. *Please see our supplement for more distillation details.*

To elaborate, we test all distilled models with the same 4-step sampling, which is shown to be able to achieve the best sampling performance; we then compare each distilled model with the undistilled one on the normalized sampling cost. We follow the same practice discussed in Section 3.3 for selecting the optimal CFG rate and compare them under the same relative inference cost. The results shown in the left part of Fig. 13 demonstrate that distillation significantly improves the generative performance for all models in 4-step sampling, with FID improvements across the board. By comparing these distilled models with the undistilled models in the right part of Fig. 13, we demonstrate that distilled models outperform undistilled models at the same sampling cost. However, at the specific sampling cost, *i.e.*, sampling cost ≈ 8 , the smaller undistilled 83M model still achieves similar performance to the larger distilled 866M model. The observation further supports our proposed scaling sampling-efficiency of LDMs, which still holds under the circumstance of diffusion distillation.

4 Conclusion

In this paper, we investigated scaling properties of Latent Diffusion Models (LDMs), specifically through scaling model size from 39 million to 5 billion parameters. We trained these scaled models from scratch on a large-scale text-to-image dataset and then finetuned the pretrained models for downstream tasks. Our findings unveil that, under identical sampling costs, smaller models frequently outperform larger models, suggesting a promising direction for accelerating LDMs in terms of model size. We further show that the sampling efficiency is consistent in multiple axes. For example, it is invariant to various diffusion samplers (stochastic and deterministic), and also holds true for distilled models. We believe this analysis of scaling sampling efficiency would be instrumental in guiding future developments of LDMs, specifically for balancing model size against performance and efficiency in a broad spectrum of practical applications.

Limitations. This work utilizes visual quality inspection alongside established metrics like FID and CLIP scores. We opted to avoid human evaluations due to the immense number of different combinations needed for the more than 1000 variants considered in this study. However, it is important to acknowledge the potential discrepancy between visual quality and quantitative metrics, which is actively discussed in recent works [7, 19, 73]. Furthermore, claims regarding the scalability of latent models are made specifically for the particular model family

studied in this work. Extending this analysis to other model families, particularly those incorporating transformer-based backbones [38,43,47], would be a valuable direction for future research.

5 Acknowledgments

We are grateful to Keren Ye, Jason Baldridge for their valuable feedback. We also extend our gratitude to Shlomi Fruchter, Kevin Murphy, Mohammad Babaeizadeh, and Han Zhang for their instrumental contributions in facilitating the initial implementation of the latent diffusion models.

References

1. Alabdulmohsin, I.M., Zhai, X., Kolesnikov, A., Beyer, L.: Getting vit in shape: Scaling laws for compute-optimal model design. *Advances in Neural Information Processing Systems* (2024) 3
2. Anil, R., Dai, A.M., Firat, O., Johnson, M., Lepikhin, D., Passos, A., Shakeri, S., Taropa, E., Bailey, P., Chen, Z., et al.: Palm 2 technical report. *ArXiv preprint* (2023) 3
3. Brown, T.B., Mann, B., Ryder, N., Subbiah, M., Kaplan, J., Dhariwal, P., Neelakantan, A., Shyam, P., Sastry, G., Askell, A., Agarwal, S., Herbert-Voss, A., Krueger, G., Henighan, T., Child, R., Ramesh, A., Ziegler, D.M., Wu, J., Winter, C., Hesse, C., Chen, M., Sigler, E., Litwin, M., Gray, S., Chess, B., Clark, J., Berner, C., McCandlish, S., Radford, A., Sutskever, I., Amodei, D.: Language models are few-shot learners. In: *Advances in Neural Information Processing Systems 33: Annual Conference on Neural Information Processing Systems 2020, NeurIPS 2020, December 6-12, 2020, virtual* (2020) 3
4. Chang, H., Zhang, H., Barber, J., Maschinot, A., Lezama, J., Jiang, L., Yang, M.H., Murphy, K., Freeman, W.T., Rubinstein, M., et al.: Muse: Text-to-image generation via masked generative transformers. *ArXiv preprint* (2023) 4
5. Chang, H., Zhang, H., Jiang, L., Liu, C., Freeman, W.T.: Maskgit: Masked generative image transformer. In: *IEEE/CVF Conference on Computer Vision and Pattern Recognition, CVPR 2022, New Orleans, LA, USA, June 18-24, 2022* (2022) 4
6. Chen, M., Radford, A., Child, R., Wu, J., Jun, H., Luan, D., Sutskever, I.: Generative pretraining from pixels. In: *Proceedings of the 37th International Conference on Machine Learning, ICML 2020, 13-18 July 2020, Virtual Event. Proceedings of Machine Learning Research* (2020) 3
7. Cho, J., Hu, Y., Garg, R., Anderson, P., Krishna, R., Baldridge, J., Bansal, M., Pont-Tuset, J., Wang, S.: Davidsonian scene graph: Improving reliability in fine-grained evaluation for text-image generation. *ArXiv preprint* (2023) 14
8. Choi, J., Kim, M., Ahn, D., Kim, T., Kim, Y., Jo, D., Jeon, H., Kim, J.J., Kim, H.: Squeezing large-scale diffusion models for mobile. *ArXiv preprint* (2023) 1, 2, 4
9. Delbracio, M., Milanfar, P.: Inversion by direct iteration: An alternative to denoising diffusion for image restoration. *Transactions on Machine Learning Research* (2023), featured Certification 1

10. Devlin, J., Chang, M.W., Lee, K., Toutanova, K.: BERT: Pre-training of deep bidirectional transformers for language understanding. In: Proceedings of the 2019 Conference of the North American Chapter of the Association for Computational Linguistics: Human Language Technologies, Volume 1 (Long and Short Papers) (2019) [4](#)
11. Dockhorn, T., Vahdat, A., Kreis, K.: Genie: Higher-order denoising diffusion solvers. *Advances in Neural Information Processing Systems* (2022) [2](#), [4](#)
12. Du, H., Zhang, R., Niyato, D., Kang, J., Xiong, Z., Kim, D.I., Shen, X.S., Poor, H.V.: Exploring collaborative distributed diffusion-based ai-generated content (aigc) in wireless networks. *IEEE Network* (99) (2023) [1](#)
13. Goodfellow, I., Pouget-Abadie, J., Mirza, M., Xu, B., Warde-Farley, D., Ozair, S., Courville, A., Bengio, Y.: Generative adversarial networks. *Communications of the ACM* (11) (2020) [2](#), [4](#)
14. Gu, J., Zhai, S., Zhang, Y., Liu, L., Susskind, J.M.: Boot: Data-free distillation of denoising diffusion models with bootstrapping. In: ICML 2023 Workshop on Structured Probabilistic Inference $\{\&\}$ Generative Modeling (2023) [2](#), [14](#)
15. He, K., Chen, X., Xie, S., Li, Y., Dollár, P., Girshick, R.B.: Masked autoencoders are scalable vision learners. In: IEEE/CVF Conference on Computer Vision and Pattern Recognition, CVPR 2022, New Orleans, LA, USA, June 18-24, 2022 (2022) [4](#)
16. Ho, J., Jain, A., Abbeel, P.: Denoising diffusion probabilistic models. In: *Advances in Neural Information Processing Systems 33: Annual Conference on Neural Information Processing Systems 2020, NeurIPS 2020, December 6-12, 2020, virtual* (2020) [1](#), [3](#), [12](#)
17. Ho, J., Salimans, T.: Classifier-free diffusion guidance. *ArXiv preprint* (2022) [9](#)
18. Hoffmann, J., Borgeaud, S., Mensch, A., Buchatskaya, E., Cai, T., Rutherford, E., Casas, D.d.L., Hendricks, L.A., Welbl, J., Clark, A., et al.: Training compute-optimal large language models. *ArXiv preprint* (2022) [3](#)
19. Jayasumana, S., Ramalingam, S., Veit, A., Glasner, D., Chakrabarti, A., Kumar, S.: Rethinking fid: Towards a better evaluation metric for image generation. *ArXiv preprint* (2024) [14](#)
20. Jouppi, N., Kurian, G., Li, S., Ma, P., Nagarajan, R., Nai, L., Patil, N., Subramanian, S., Swing, A., Towles, B., et al.: Tpu v4: An optically reconfigurable supercomputer for machine learning with hardware support for embeddings. In: *Proceedings of the 50th Annual International Symposium on Computer Architecture* (2023) [2](#)
21. Kaplan, J., McCandlish, S., Henighan, T., Brown, T.B., Chess, B., Child, R., Gray, S., Radford, A., Wu, J., Amodei, D.: Scaling laws for neural language models. *ArXiv preprint* (2020) [3](#)
22. Karras, T., Aittala, M., Aila, T., Laine, S.: Elucidating the design space of diffusion-based generative models. *Advances in Neural Information Processing Systems* (2022) [2](#), [4](#)
23. Karras, T., Laine, S., Aila, T.: A style-based generator architecture for generative adversarial networks. In: *IEEE Conference on Computer Vision and Pattern Recognition, CVPR 2019, Long Beach, CA, USA, June 16-20, 2019* (2019) [2](#), [4](#)
24. Kim, B.K., Song, H.K., Castells, T., Choi, S.: Bk-sdm: Architecturally compressed stable diffusion for efficient text-to-image generation. In: *Workshop on Efficient Systems for Foundation Models@ ICML2023* (2023) [2](#), [4](#)
25. Kim, B.K., Song, H.K., Castells, T., Choi, S.: On architectural compression of text-to-image diffusion models. *ArXiv preprint* (2023) [2](#), [4](#)

26. Kingma, D.P., Welling, M.: Auto-encoding variational bayes. In: 2nd International Conference on Learning Representations, ICLR 2014, Banff, AB, Canada, April 14-16, 2014, Conference Track Proceedings (2014) [4](#)
27. Li, Y., Wang, H., Jin, Q., Hu, J., Chemerys, P., Fu, Y., Wang, Y., Tulyakov, S., Ren, J.: Snapfusion: Text-to-image diffusion model on mobile devices within two seconds. ArXiv preprint (2023) [2](#), [4](#)
28. Lin, C.H., Gao, J., Tang, L., Takikawa, T., Zeng, X., Huang, X., Kreis, K., Fidler, S., Liu, M.Y., Lin, T.Y.: Magic3d: High-resolution text-to-3d content creation. In: Proceedings of the IEEE/CVF Conference on Computer Vision and Pattern Recognition (2023) [1](#)
29. Lin, S., Wang, A., Yang, X.: Sdxl-lightning: Progressive adversarial diffusion distillation. ArXiv preprint (2024) [14](#)
30. Lin, T.Y., Maire, M., Belongie, S., Hays, J., Perona, P., Ramanan, D., Dollár, P., Zitnick, C.L.: Microsoft coco: Common objects in context. In: ECCV (2014) [1](#), [6](#)
31. Liu, H., Chen, Z., Yuan, Y., Mei, X., Liu, X., Mandic, D., Wang, W., Plumbley, M.D.: Audioldm: Text-to-audio generation with latent diffusion models. ArXiv preprint (2023) [1](#)
32. Liu, R., Wu, R., Van Hoorick, B., Tokmakov, P., Zakharov, S., Vondrick, C.: Zero-1-to-3: Zero-shot one image to 3d object. In: Proceedings of the IEEE/CVF International Conference on Computer Vision (2023) [1](#)
33. Liu, X., Zhang, X., Ma, J., Peng, J., Liu, Q.: Instaflow: One step is enough for high-quality diffusion-based text-to-image generation. ArXiv preprint (2023) [2](#), [4](#)
34. Lu, C., Zhou, Y., Bao, F., Chen, J., Li, C., Zhu, J.: Dpm-solver: A fast ode solver for diffusion probabilistic model sampling in around 10 steps. Advances in Neural Information Processing Systems (2022) [2](#), [4](#)
35. Lu, C., Zhou, Y., Bao, F., Chen, J., Li, C., Zhu, J.: Dpm-solver++: Fast solver for guided sampling of diffusion probabilistic models. ArXiv preprint (2022) [3](#), [12](#)
36. Luhman, E., Luhman, T.: Knowledge distillation in iterative generative models for improved sampling speed. ArXiv preprint (2021) [2](#), [14](#)
37. Luo, S., Tan, Y., Huang, L., Li, J., Zhao, H.: Latent consistency models: Synthesizing high-resolution images with few-step inference. ArXiv preprint (2023) [14](#)
38. Ma, N., Goldstein, M., Albergo, M.S., Boffi, N.M., Vanden-Eijnden, E., Xie, S.: Sit: Exploring flow and diffusion-based generative models with scalable interpolant transformers. ArXiv preprint (2024) [15](#)
39. Makhzani, A., Shlens, J., Jaitly, N., Goodfellow, I., Frey, B.: Adversarial autoencoders. ArXiv preprint (2015) [4](#)
40. Mao, X., Li, Q., Xie, H., Lau, R.Y.K., Wang, Z., Smolley, S.P.: Least squares generative adversarial networks. In: IEEE International Conference on Computer Vision, ICCV 2017, Venice, Italy, October 22-29, 2017 (2017) [4](#)
41. Mei, K., Delbracio, M., Talebi, H., Tu, Z., Patel, V.M., Milanfar, P.: Codi: Conditional diffusion distillation for higher-fidelity and faster image generation. In: Proceedings of the IEEE/CVF Conference on Computer Vision and Pattern Recognition (2024) [2](#), [3](#), [14](#), [24](#)
42. Mei, K., Patel, V.: Vidm: Video implicit diffusion models. In: Proceedings of the AAAI Conference on Artificial Intelligence. No. 8 (2023) [1](#)
43. Mei, K., Zhou, M., Patel, V.M.: T1: Scaling diffusion probabilistic fields to high-resolution on unified visual modalities. ArXiv preprint (2023) [1](#), [15](#)
44. Meng, C., Rombach, R., Gao, R., Kingma, D., Ermon, S., Ho, J., Salimans, T.: On distillation of guided diffusion models. In: Proceedings of the IEEE/CVF Conference on Computer Vision and Pattern Recognition (2023) [24](#)

45. Miyato, T., Kataoka, T., Koyama, M., Yoshida, Y.: Spectral normalization for generative adversarial networks. In: 6th International Conference on Learning Representations, ICLR 2018, Vancouver, BC, Canada, April 30 - May 3, 2018, Conference Track Proceedings (2018) [4](#)
46. Nichol, A.Q., Dhariwal, P.: Improved denoising diffusion probabilistic models. In: Proceedings of the 38th International Conference on Machine Learning, ICML 2021, 18-24 July 2021, Virtual Event. Proceedings of Machine Learning Research (2021) [3](#)
47. Peebles, W., Xie, S.: Scalable diffusion models with transformers. In: Proceedings of the IEEE/CVF International Conference on Computer Vision (2023) [2](#), [3](#), [4](#), [15](#)
48. Podell, D., English, Z., Lacey, K., Blattmann, A., Dockhorn, T., Müller, J., Penna, J., Rombach, R.: Sdxl: Improving latent diffusion models for high-resolution image synthesis. ArXiv preprint (2023) [1](#), [4](#)
49. Qi, C., Tu, Z., Ye, K., Delbracio, M., Milanfar, P., Chen, Q., Talebi, H.: Tip: Text-driven image processing with semantic and restoration instructions. ArXiv preprint (2023) [1](#)
50. Raffel, C., Shazeer, N., Roberts, A., Lee, K., Narang, S., Matena, M., Zhou, Y., Li, W., Liu, P.J.: Exploring the limits of transfer learning with a unified text-to-text transformer. *J. Mach. Learn. Res.* (2020) [4](#)
51. Ramesh, A., Dhariwal, P., Nichol, A., Chu, C., Chen, M.: Hierarchical text-conditional image generation with clip latents. ArXiv preprint (2022) [4](#)
52. Reed, S.E., Akata, Z., Yan, X., Logeswaran, L., Schiele, B., Lee, H.: Generative adversarial text to image synthesis. In: Proceedings of the 33rd International Conference on Machine Learning, ICML 2016, New York City, NY, USA, June 19-24, 2016. JMLR Workshop and Conference Proceedings (2016) [4](#)
53. Ren, M., Delbracio, M., Talebi, H., Gerig, G., Milanfar, P.: Multiscale structure guided diffusion for image deblurring. In: Proceedings of the IEEE/CVF International Conference on Computer Vision (2023) [1](#)
54. Rezende, D.J., Mohamed, S.: Variational inference with normalizing flows. In: Proceedings of the 32nd International Conference on Machine Learning, ICML 2015, Lille, France, 6-11 July 2015. JMLR Workshop and Conference Proceedings (2015) [4](#)
55. Rombach, R., Blattmann, A., Lorenz, D., Esser, P., Ommer, B.: High-resolution image synthesis with latent diffusion models. In: Proceedings of the IEEE/CVF conference on computer vision and pattern recognition (2022) [1](#), [3](#), [4](#), [9](#)
56. Ruiz, N., Li, Y., Jampani, V., Pritch, Y., Rubinstein, M., Aberman, K.: Dreambooth: Fine tuning text-to-image diffusion models for subject-driven generation. In: Proceedings of the IEEE/CVF Conference on Computer Vision and Pattern Recognition (2023) [2](#), [3](#), [7](#)
57. Sahak, H., Watson, D., Saharia, C., Fleet, D.: Denoising diffusion probabilistic models for robust image super-resolution in the wild. ArXiv preprint (2023) [2](#), [7](#)
58. Saharia, C., Ho, J., Chan, W., Salimans, T., Fleet, D.J., Norouzi, M.: Image super-resolution via iterative refinement. *IEEE Transactions on Pattern Analysis and Machine Intelligence* (4) (2022) [2](#), [7](#)
59. Salimans, T., Ho, J.: Progressive distillation for fast sampling of diffusion models. In: The Tenth International Conference on Learning Representations, ICLR 2022, Virtual Event, April 25-29, 2022 (2022) [2](#), [14](#), [24](#)
60. Sauer, A., Karras, T., Laine, S., Geiger, A., Aila, T.: Stylegan-t: Unlocking the power of gans for fast large-scale text-to-image synthesis. ArXiv preprint (2023) [4](#)
61. Sauer, A., Lorenz, D., Blattmann, A., Rombach, R.: Adversarial diffusion distillation. ArXiv preprint (2023) [2](#), [14](#)

62. Schuhmann, C., Beaumont, R., Vencu, R., Gordon, C., Wightman, R., Cherti, M., Coombes, T., Katta, A., Mullis, C., Wortsman, M., et al.: Laion-5b: An open large-scale dataset for training next generation image-text models. *Advances in Neural Information Processing Systems* (2022) [1](#)
63. Singer, U., Polyak, A., Hayes, T., Yin, X., An, J., Zhang, S., Hu, Q., Yang, H., Ashual, O., Gafni, O., et al.: Make-a-video: Text-to-video generation without text-video data. *ArXiv preprint* (2022) [1](#)
64. Song, J., Meng, C., Ermon, S.: Denoising diffusion implicit models. In: *9th International Conference on Learning Representations, ICLR 2021, Virtual Event, Austria, May 3-7, 2021* (2021) [1](#), [2](#), [3](#), [4](#)
65. Song, Y., Dhariwal, P., Chen, M., Sutskever, I.: Consistency models (2023) [2](#), [14](#), [24](#)
66. Song, Y., Sohl-Dickstein, J., Kingma, D.P., Kumar, A., Ermon, S., Poole, B.: Score-based generative modeling through stochastic differential equations. In: *9th International Conference on Learning Representations, ICLR 2021, Virtual Event, Austria, May 3-7, 2021* (2021) [1](#)
67. Touvron, H., Martin, L., Stone, K., Albert, P., Almahairi, A., Babaei, Y., Bashlykov, N., Batra, S., Bhargava, P., Bhosale, S., et al.: Llama 2: Open foundation and fine-tuned chat models. *ArXiv preprint* (2023) [3](#)
68. Vahdat, A., Kautz, J.: NVAE: A deep hierarchical variational autoencoder. In: *Advances in Neural Information Processing Systems 33: Annual Conference on Neural Information Processing Systems 2020, NeurIPS 2020, December 6-12, 2020, virtual* (2020) [4](#)
69. Wang, X., Xie, L., Dong, C., Shan, Y.: Real-esrgan: Training real-world blind super-resolution with pure synthetic data. In: *IEEE/CVF International Conference on Computer Vision Workshops, ICCVW 2021, Montreal, BC, Canada, October 11-17, 2021* (2021) [3](#), [6](#)
70. Wu, J.Z., Ge, Y., Wang, X., Lei, S.W., Gu, Y., Shi, Y., Hsu, W., Shan, Y., Qie, X., Shou, M.Z.: Tune-a-video: One-shot tuning of image diffusion models for text-to-video generation. In: *Proceedings of the IEEE/CVF International Conference on Computer Vision* (2023) [1](#)
71. Xu, Y., Zhao, Y., Xiao, Z., Hou, T.: Ufogen: You forward once large scale text-to-image generation via diffusion gans. *ArXiv preprint* (2023) [2](#), [4](#)
72. Yu, J., Xu, Y., Koh, J.Y., Luong, T., Baid, G., Wang, Z., Vasudevan, V., Ku, A., Yang, Y., Ayan, B.K., et al.: Scaling autoregressive models for content-rich text-to-image generation. *ArXiv preprint* (2022) [5](#)
73. Zhang, H., Koh, J.Y., Baldridge, J., Lee, H., Yang, Y.: Cross-modal contrastive learning for text-to-image generation. In: *IEEE Conference on Computer Vision and Pattern Recognition, CVPR 2021, virtual, June 19-25, 2021* (2021) [14](#)
74. Zhao, Y., Xu, Y., Xiao, Z., Hou, T.: Mobicdiffusion: Subsecond text-to-image generation on mobile devices. *ArXiv preprint* (2023) [2](#), [4](#)
75. Zhou, Y., Du, N., Huang, Y., Peng, D., Lan, C., Huang, D., Shakeri, S., So, D., Dai, A.M., Lu, Y., et al.: Brainformers: Trading simplicity for efficiency. In: *International Conference on Machine Learning*. PMLR (2023) [3](#)

A Scaling the text-to-image performance

In order to provide detailed visual comparisons for Fig. 1 in the main manuscript, Fig. 14, Fig. 15, and Fig. 16 show the generated results with the same prompt and the same sampling parameters (*i.e.*, 50-step DDIM sampling and 7.5 CFG rate).

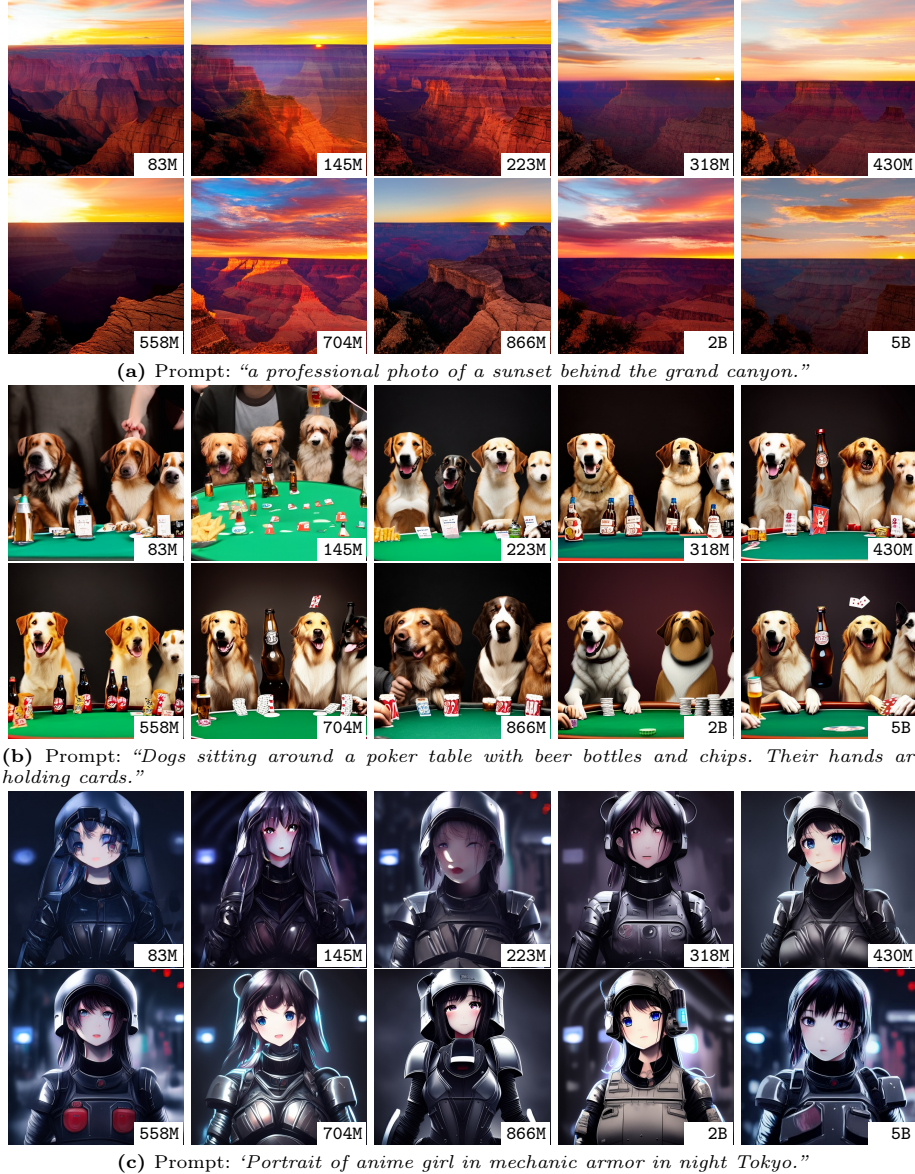


Fig. 14: Text-to-image results from our scaled LDMs (83M - 5B), highlighting the improvement in visual quality with increased model size.

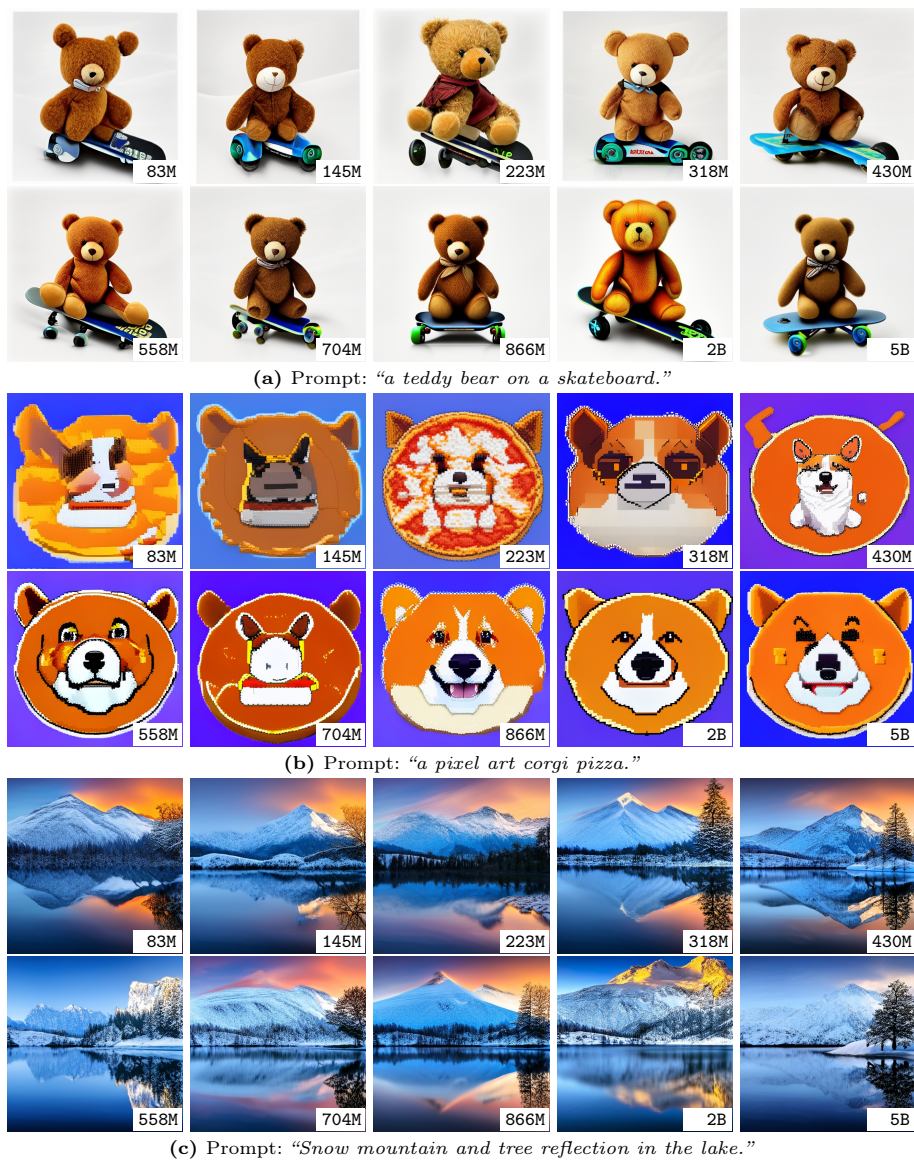


Fig. 15: Text-to-image results from our scaled LDMs (83M - 5B), highlighting the improvement in visual quality with increased model size.



(a) Prompt: “a propaganda poster depicting a cat dressed as french emperor napoleon holding a piece of cheese.”



(b) Prompt: “a store front that has the word ‘LDMs’ written on it.”



(c) Prompt: “ten red apples.”

Fig. 16: Text-to-image results from our scaled LDMs (83M - 5B), highlighting the improvement in visual quality with increased model size.

B Scaling downstream performance

To provide more metrics for the super-resolution experiments in Fig. 4 of the main manuscript, Fig. 18 shows the generative metric IS for the super-resolution results. Fig. 18 shows the visual results of the super-resolution results in order to provide more visual results for the visual comparisons of Fig. 5 in the main manuscript.

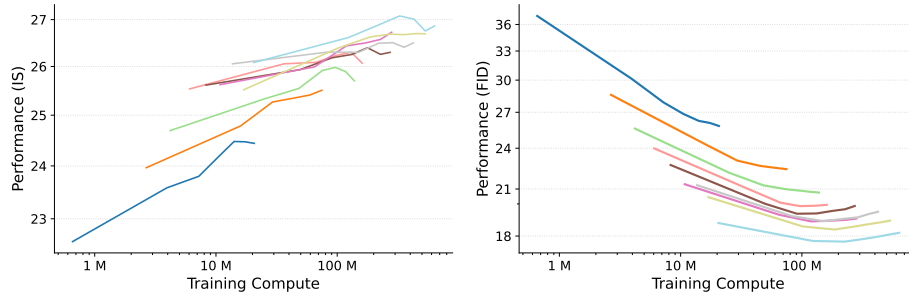


Fig. 17: For super-resolution, we show the trends between the generative metric IS and the training compute still depend on the pretraining, which is similar to the trends between the generative metric FID and the training compute.

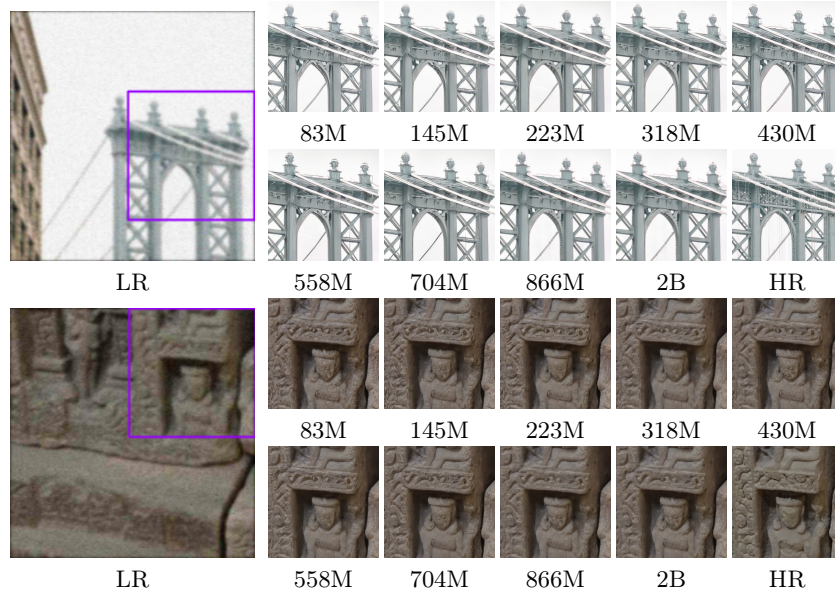


Fig. 18: In 4× super-resolution, visual quality directly improves with increased model size. As these scaled models vary in pretraining performance, the results clearly demonstrate that pretraining boosts super-resolution capabilities.

C Scaling sampling-efficiency in distilled LDMs

Diffusion distillation methods for accelerating sampling are generally derived from Progressive Distillation (PD) [59] and Consistency Models (CM) [65]. In the main paper, we have shown that CoDi [41] based on CM is scalable to different model sizes. Here we show other investigated methods, *i.e.*, guided distillation [44], has inconsistent acceleration effects across different model sizes. Fig. 19 shows guided distillation results for the 83M and 223M models respectively, where *s16* and *s8* denote different distillation stages. It is easy to see that the performance improvement of these two models is inconsistent.

Fig. 20 shows the visual results of the CoDi distilled models and the undistilled models under the same sampling cost to demonstrate the sampling-efficiency.

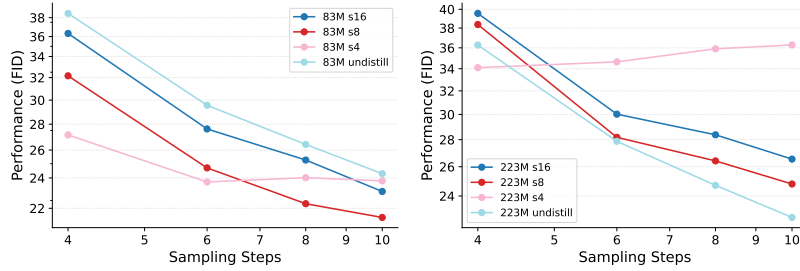


Fig. 19: *Left:* Guided distillation on the 83M model for text-to-image generation. *Right:* Guided distillation on the 224M model for text-to-image generation.



Fig. 20: We visualize text-to-image generation results of the tested LDMs under approximately the same inference cost.

D Scaling the sampling-efficiency

To provide more visual comparisons additional to Fig. 10 in the main paper, Fig. 21, Fig. 22, and Fig. 23 present visual comparisons between different scaled models under a uniform sampling cost. This highlights that the performance of smaller models can indeed match their larger counterparts under similar sampling cost.



(a) Prompt: “a cat drinking a pint of beer.”. Sampling Cost ≈ 10 .



(b) Prompt: “a teddy bear on a skateboard.”. Sampling Cost ≈ 10 .

Fig. 21: We visualize text-to-image generation results of the tested LDMs under approximately the same inference cost. We observe that smaller models can produce comparable or even better visual results than larger models under similar sampling cost (model GFLOPs \times sampling steps).

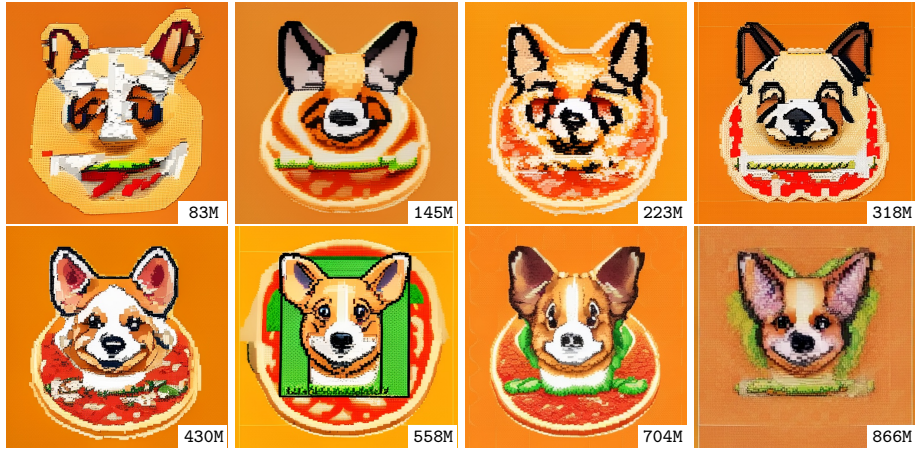


(a) Prompt: “a propaganda poster depicting a cat dressed as french emperor napoleon holding a piece of cheese.”. Sampling Cost ≈ 14 .



(b) Prompt: “Dogs sitting around a poker table with beer bottles and chips.”. Sampling Cost ≈ 14 .

Fig. 22: We visualize text-to-image generation results of the tested LDMs under approximately the same inference cost. We observe that smaller models can produce comparable or even better visual results than larger models under similar sampling cost (model GFLOPs \times sampling steps).



(a) Prompt: “a pixel art corgi pizza.”. Sampling Cost ≈ 18 .



(b) Prompt: “Snow mountain and tree reflection in the lake.”. Sampling Cost ≈ 18 .

Fig. 23: We visualize text-to-image generation results of the tested LDMS under approximately the same inference cost. We observe that smaller models can produce comparable or even better visual results than larger models under similar sampling cost (model GFLOPs \times sampling steps).